Analysis of waves subjected to mechanical force and voids source in an initially stressed magneto-elastic medium with corrugated and impedance boundary

Augustine Igwebuike Anya

GST-Mathematics Division, Veritas University Abuja, Bwari-Abuja, Nigeria

Corresponding Author's Emails: anyaa@veritas.edu.ng, anyaaugustineigwebuike@gmail.com
Mobile number: +2347038933954

Abstract

The analysis of surface waves in an initially stressed homogeneous magneto-elastic material with voids source, corrugated and impedance boundary conditions influenced by an applied mechanical force on the surface of the material is the hallmark of this investigation. The framework of the study also encompasses the use of normal mode solution approach, non-dimensionalization of the resulting equations of motion and grooved boundary conditions occasioned by the modeled problem. The distribution of the displacement components, normal and shear stresses, volume fraction fields were analytically and graphically presented using Mathematica Software for a particular chosen material which hitherto demonstrates the effects of the contributing physical quantities on the material. The initial stress, voids source, and Mechanical force have remarkable effects to the behavior of the distribution profiles on the material. Increased influences of the magnetic fields decrease the amplitude of the distribution functions whereas impedance parameter induced a mechanical like resistance to the distributions. Thus, this work should prove useful in understanding studies involving seismology. Also, researchers in the fields of Geophysics, Mathematics of waves, Material Sciences, amongst others should be able to find the work helpful.

Keywords

Voids source, influence of magnetic fields, mechanical force, initial stress, fibre-reinforcement, corrugation, impedance**.**

1. Introduction

Studies in seismology have gained traction over the years due to its importance in examining disturbances in and on the earth especially as it behooves the fields of earthquake sciences, Geotechnical and Geophysics studies, and so on. Also, reading the disturbances in these materials, especially, has always been the anchor of Scientists in this field. These Scientists develop Mathematical models that could aid the understanding of wave phenomenon for various chosen materials like the fibre-reinforced composites, Spencer [1]. Fiber-reinforced composites have light weight and good stiffness property. This has culminated to their relevance over the years in several applications such as in the fields of engineering, construction and architectural designs, among others. Hence, the need for reinforcement of structures and the solutions of the dispersion and attenuation characteristics of surface waves on these structures are paramount. This led Alam et al [2-3], to carry out works on Love-Type wave as one of surface waves on a fiber-reinforced composite over a viscoelastic substrate. There works equally dealt on the SH-waves in a temperature-dependent Voigt-type viscoelastic strip over an inhomogeneous half-space. In furthering these works on composites, Bounouara et al [4], examined the effect of visco-Pasternak foundation on thermo-mechanical bending response of anisotropic thick laminated composite plates. Further similar work was equally carried out by Mario et al [5], in their quest to finding SH-wave solutions for a multi-layered model of Newtonian viscous liquid, fiber-reinforcement and poro-elasticity. Generally, it is to be noted that composite materials share similar material properties with orthotropic materials like the wood.

More so, due to many physical causes, some given physical properties and parameters such as initially stressed material like the earth Biot [6], and magnetic fields are sometimes inculcated into the material characterization Abd-Alla et al [7]. In addition to this, Alam et al [8] and Alam et al [9], rightly utilized such physical parameters and characterization of materials in their studies of attenuation and dispersion of waves in anelastic and elastic strips with porosity, and that which relates the rotating radial vibrations in human bones made cylindrical shell under magnetic field and hydrostatic stress, respectively. These are in order to elicit the understanding of the behaviors associated with these materials that are subject to an impact and in turn resulting to propagation of elastic waves. This was similarly observed by Cowin et al [10], whose works covered voids (volume fraction fields or porosity) as an important generalization to mechanical characteristics of materials. Thus, in studying the Love-type wave propagation due to an impulsive point source, Venkatesan et al [11], was able to find solution in his work for a Multi-layered model of poroelastic cum inhomogeneous media using the Green's function approach. Tahir et al [12-13], equally proceeded to opine the solutions to the propagation analysis of a ceramic-metal functionally graded sandwich plate with different porosity distributions in a hygro-thermal environment and for functionally graded sandwich plates via a simple quasi-3D HSDT. Also, Alsubaie et al [14], contributed in deciphering information about porosity-dependent vibration in functionally graded carbon nanotube-reinforced composite beam.
Furthermore, it's evident that boundary surfaces of some materials are plane, grooved/corrugated or entirely of different shapes in nature. Grooved boundary surface could be visualized as series of parallel furrows and ridges whose encounter in mechanical propagation of wave results to several effects especially across interfaces, Asano [15]. It is worthy to mention that several related works has been carried out by some authors on irregular boundary surface. Chowdhury et al [16] is one of such authors whose study covered solutions on irregular common interface of two hydrostatic stressed media. In a similar vein, Sadab et al [17-18], equally examined such kind of model in their investigation about SH-wave propagation in double layers imperfectly bonded media, and also in their work for piezoelectric layer over a heterogeneous dry sandy material.
Be that as it may, impedance boundary conditions are a linear combination of unknown functions and their derivatives prescribed on the boundary, Singh [19]. These kinds of boundary conditions are commonly used in various fields such as in electromagneto-acoustics phenomena. They are usually not in vogue in seismology even though one could speak of the existence of virtually various boundaries in the earth's interior. Frankly speaking, the contact between two solid media represents a complex phenomenon. For instance, in the case of seismic wave contacts with discontinuities, an ideally well bonded contact is assumed to include the continuity of appropriate stress and displacement components on the media. Thus, it is appropriate to assume such contact planes as very thin layers which could lead to impedance-like boundary conditions on the surface of the structure. In the quest for solutions involving impedance, Maleki et al [20] constructed model tests on determining the effect of various geometrical aspects on horizontal impedance function of surface footings.
In spite of this, some other authors have also made contributions to these concepts of corrugated boundary and other related wave propagation phenomena; Singh et al [21-23], Das et al [24], Abd-Alla et al [25], Chattopadhyay et al [26], Roy et al [27], Singh et al [28], Gupta et al [29-30], Anya et al [31-34], Sunita et al [35], Dey et al [36], Nunziato et al [37] and Puri et al [38], Singh et al[39-40], Sahu et al [41], Giovannini [42] and Rakshit et al [43-44], most especially as an individual or part considerations of the interacting physical quantities rather than in a combined effect as observed in this current examination.

In considerations of the above literatures, this study is aimed at deriving a Mathematical model of waves that could aid the understanding of the analysis of surface waves in an initially stressed homogeneous magneto-elastic material with voids source, corrugated and impedance boundary conditions influenced by an applied mechanical force. Consequently, this tend to be advantageous and imperative to investigate owing to the nature of the considered physical structure and its characterization in solid mechanics of materials, Mathematics of waves phenomena and generally, seismic solutions. Thus, the chosen boundary conditions of corrugation and impedance occasioned by the voids source and mechanical force, forms a huge contributions in combined form to the result of the current study on composites. Hence, the equations of motion are derived by incorporating magnetic fields and initial stress to field equations of the material characterization. And by the utilization of normal mode analysis and non-dimensionalized quantities of the resulting equations of motion and grooved boundary conditions, the analytical and graphical solutions are presented for the displacement components, volume fraction fields and stresses on the structure. We observed that the physical parameters used in this study has varying degrees of effect on the distribution component of displacements of the waves, volume fraction fields and stresses on the material.

2. The Mathematical Formulations

We present the constitutive equations for an initially stressed magneto-porous fibre–reinforced composites, Spencer [1], Biot [6], Abd–Alla et al [7], Anya et al [31], Singh[45], and Othman et al [46] by:

$$\tau_{ij} = -P\left(\delta_{ij} + \varpi_{ij}\right) + \lambda\varepsilon_{kk}\delta_{ij} + 2\mu_T\varepsilon_{ij} + \alpha(a_k a_m \varepsilon_{km}\delta_{ij} + \varepsilon_{kk}a_i a_j) + 2(\mu_L - \mu_T)(a_i a_k \varepsilon_{kj} + a_j a_k \varepsilon_{ki}) \\ + \beta(a_k a_m \varepsilon_{km} a_i a_j) + \xi\delta_{ij}\phi, \tag{1}$$

$$F_i = \mu_0 H_0^2 \left(e_{,1} - \varepsilon_0 \mu_0 \ddot{u}_1, e_{,2} - \varepsilon_0 \mu_0 \ddot{u}_2, 0\right), \tag{2}$$

where, $e = (u_{1,1} + u_{2,2})$, $\varpi_{ij} = \frac{1}{2}\left(u_{i,j} - u_{j,i}\right)$ is the rigid body rotation tensor, and $\varepsilon_{ij} = \frac{1}{2}\left(u_{i,j} + u_{j,i}\right)$. τ_{ij}, ε_{ij}, δ_{ij}, λ, $(\alpha,\ \beta,\ (\mu_L - \mu_T))$, u_i, ϕ P, and F_i are the stress tensor, strain tensor, Kronecker–delta function, Lames constant, fiber-reinforced parameters, displacement components, volume fraction fields, initially stressed parameter, and magnetic force respectively, $i = j = 1,2,3.$ Take $H_i = H_0\delta_{i3} + h_i$, and h_i as the induced magnetic field. ε_o is the electric permeability such that the solid medium lies in the x_1x_2- plane. $h_i\left(x_1, x_2, x_3\right) = -u_{k,k}\delta_{i3}$. H_i is the magnetic vector field while μ_o is the magnetic permeability as adapted from Maxwell's equations of electromagnetism. Also, we assume $a = (a_1, a_2, a_3)$ such that $a = (1,0,0)$ represents the fibre directions. Consequently, the field equations in the presence of magnetic, Abd–Alla et al [7] and volume fraction fields, Cowin et al [10], take the forms:

$$\tau_{ij,j} + F_i = \rho\ddot{u}_i, \tag{3}$$

$$\xi_1(\phi_{,ii}) - \omega_o\phi - \varpi\dot{\phi} - \xi(u_{i,i}) = \rho\kappa\ddot{\phi}. \tag{4}$$

In view of the above formulations, we restrict our analysis to a 2D problem in the x_1x_2- plane such that $x_3 = 0$ and $x_1 \neq x_2 \neq 0,$ since the displacement u_3 is uncoupled in the equation of motion whereas the displacements $u_1 \neq u_2 \neq 0$ are coupled. Thus, the component forms of Equations (3–4); are presented below:

$$A_1 u_{1,11} + A_2 u_{2,21} + A_3 u_{1,22} = \{\rho + \varepsilon_0\mu_0^2 H_0^2\}\ddot{u}_1 - \xi\phi_{,1}, \tag{5}$$

$$A_2 u_{1,12} + A_4 u_{2,11} + A_5 u_{2,22} = \{\rho + \varepsilon_0\mu_0^2 H_0^2\}\ddot{u}_2 - \xi\phi_{,2}, \tag{6}$$

$$\xi_1(\phi_{,ii}) - \omega_o\phi - \varpi\dot{\phi} - \xi(u_{i,i}) = \rho\kappa\ddot{\phi}. \tag{7}$$

Here,

$A_1 = (\lambda + 2\alpha + 4\mu_L - 2\mu_T + \beta + \mu_0 H_0^2), A_2 = (\alpha + \lambda + \mu_L + \mu_0 H_0^2 + P/2), A_3 = \mu_L - P/2,$
$A_4 = \mu_L - P/2, A_5 = (\lambda + 2\mu_T + \mu_0 H_0^2).$

The following dimensionless constants; $(t') = c_0^2$ t, $\phi' = \phi, (x_1', x_2', u_1', u_2') = c_0(x_1, x_2, u_1, u_2),$ $\tau_{ij}' = \tau_{ij} / \rho c_0^2, c_0^2 = A_1 / \rho,$ are introduced into Equations (5-7). Dropping the sign "$'$", the resulting equations of motion yields:

$$u_{1,11} + A_{12} u_{2,21} + A_{13} u_{1,22} + A_{11} \phi_{,1} = \{1 + \varepsilon_0 \mu_0^2 H_0^2 / \rho\} \ddot{u}_1, \tag{8}$$

$$A_{12} u_{1,12} + A_{14} u_{2,11} + A_{15} u_{2,22} + A_{11} \phi_{,2} = \{1 + \varepsilon_0 \mu_0^2 H_0^2 / \rho\} \ddot{u}_2, \tag{9}$$

$$A_6(\phi_{,ii}) - A_7 \phi - A_8 \dot{\phi} - A_9(u_{i,i}) = A_{10} \ddot{\phi}. \tag{10}$$

Where; $(A_{12}, A_{13}, A_{14}, A_{15}, A_6, A_8, A_{11}) = (A_2, A_3, A_4, A_5, \xi_1, \varpi, \xi) / A_1, (A_7, A_9) = (\omega_o \rho, \xi \rho) / A_1^2,\ A_{10} = \kappa.$

3. Normal Mode Approach

Considering impedance and grooved boundary of an initially stressed porous homogeneous fibre-reinforced solid in the half-space under the influence of mechanical force and magnetic fields, we take into account that the normal mode analysis is adopted such that the wave displacements and volume fraction fields are taken as;

$$(u_j, \phi) = \{\bar{u}_j(x_2), \bar{\phi}(x_2)\} e^{\omega t + ibx_1},\ j = 1, 2. \tag{11}$$

Equations (5-7); give rise to the equations below when Equation (11); is introduced into it, i.e.

$$(A_{13} D^2 - b^2 - (1 + \varepsilon_0 \mu_0^2 H_0^2 / \rho)\omega^2)\bar{u}_1 + (iA_{12} bD)\bar{u}_2 + bi\bar{\phi} = 0, \tag{12}$$

$$(iA_{12} bD)\bar{u}_1 + (A_{15} D^2 - A_{14} b^2 - (1 + \varepsilon_0 \mu_0^2 H_0^2 / \rho)\omega^2)\bar{u}_2 + D\bar{\phi} = 0, \tag{13}$$

$$-A_9 ib\bar{u}_1 - A_9 D\bar{u}_2 + (A_6 D^2 - (A_6 b^2 + A_7 + A_8 \omega - A_{10}\omega^2))\bar{\phi} = 0. \tag{14}$$

For a non-trivial solution, the set of homogenous equations(12-14); becomes:

$$(C_1 D^6 + C_2 D^4 + C_3 D^2 + C_4)(\bar{u}_1, \bar{u}_2, \bar{\phi}) = 0. \tag{15}$$

Where $C_i, i = 1, 2, 3, 4$ are complex coefficients having attributes of the physical constants of the material. Given that $\nu_i, i = 1, 2, 3$ prescribe positive real roots of the auxiliary Equation (15); normal mode approach implies we have the following form of solution:

$$(\bar{u}_{1,} \bar{u}_2, \bar{\phi}) = \sum_{n=1}^{3} (N_n, N_{1n}, N_{2n}) e^{-\nu_n x_2}, \tag{16}$$

N_n, N_{1n} and N_{2n} depends on the wave number b in the x_1 direction and the complex frequency ω of the waves. Making use of Equation (16) into Equations (12-14); we get the relations;

$$N_{1n} = H_{1n}N_n, \tag{17}$$
$$N_{2n} = H_{2n}N_n, \tag{18}$$

where; $H_{1n} = -\{A_{12}b^2 + (A_{13}\nu_n^2 - b^2 - K_1)\}\nu_n N_n / ib\{-A_{12}\nu_n^2 + (A_{15}\nu_n^2 - A_{14}b^2 - K_1)\}$,
$H_{2n} = \{-\nu_n H_{1n} + ib\}A_9 N_n / \{(\omega(A_8 - A_{10}\omega)) + A_6(\nu_n^2 - b^2) + A_7\}, \mathrm{K}_1 = (1+\varepsilon_0\mu_0^2 H_0^2/\rho)\omega^2, n = 1,2,3.$
The solutions for the total displacement component functions and stresses on the material in the dimensionless forms are thus, obtained:

$$u_1 = \sum_{n=1}^{3} N_n e^{-\nu_n x_2 + \omega t + ibx_1},\ u_2 = \sum_{n=1}^{3} N_n H_{1n} e^{-\nu_n x_2 + \omega t + ibx_1},\ \phi = \sum_{n=1}^{3} N_n H_{2n} e^{-\nu_n x_2 + \omega t + ibx_1},$$
$$\tau_{11} = \sum_{n=1}^{3} \{ib(1 - (\mu_0 H_0^2 / A_1)) - \nu_n H_{1n} A_{16} + H_{2n}\} N_n e^{-\nu_n x_2 + \omega t + ibx_1} - P/A_1,$$
$$\tau_{22} = \sum_{n=1}^{3} \{ibA_{16} - \nu_n H_{1n} A_{17} + H_{2n}\} N_n e^{-\nu_n x_2 + \omega t + ibx_1} - P/A_1,\ \tau_{12} = \sum_{n=1}^{3} \{ibH_{1n} A_{31} - \nu_n A_{13}\} N_n e^{-\nu_n x_2 + \omega t + ibx_1},$$
$$\tau_{21} = \sum_{n=1}^{3} \{ibH_{1n} A_{13} - \nu_n A_{31}\} N_n e^{-\nu_n x_2 + \omega t + ibx_1}, A_{16} = (\lambda + \alpha)/A_1, A_{17} = (\lambda + 2\mu_T)/A_1, A_{31} = (\mu_L + P/2)/A_1.$$

4. Corrugated Boundary Conditions and Applications

We assume the corrugated boundary of the porous fibre-reinforced half-space with voids source and mechanical force is denoted by $x_2 = \eta(x_1)$, where $\eta(x_1)$ is a function which is periodic in nature and independent of x_3 such that the Trigonometric Fourier series of $\eta(x_1)$ is presented:

$$\eta(x_1) = \sum_{l=1}^{\infty} (\eta_l e^{ilbx_1} + \eta_{-l} e^{-ilbx_1}). \tag{19}$$

That is, following Asano [15], $\eta(x_1) = a\cos bx_1.$ Here a is the amplitude of the corrugated boundary, and b is the wavenumber found at the corrugated boundary surface with the wavelength $2\pi/b.$ It suffices that the boundary conditions of the modeled problem follows below.

i. The corrugated and impedance boundary conditions due to the initially stressed medium w.r.t x_2 and the associated mechanical force becomes:

$\tau_{22} - \eta'(x_1)\tau_{21} + \bar{\tau}_{22} + \omega Z_2 u_2 + P = P_1 e^{\omega t + ibx_1}$,

$\tau_{12} - \eta'(x_1)\tau_{11} + \omega Z_1 u_1 + P\varpi_{12} = 0$, at $x_2 = \eta(x_1)$, for all x_1 and t.

ii. The boundary condition due to voids and its associated voids source become:

$\xi\phi_{,2} = P_2 e^{\omega t + ibx_1}$, at $x_2 = \eta(x_1),$ respectively.

Where $\bar{\tau}_{22}$ is an additional stress on the material due to Maxwell's electromagnetism, Abd-Alla et al [7], Anya et al [31] and Azhar et al [47].
Owing to the physics of stress and impedance, the component of tangential stress τ_{12} and normal stress component τ_{22} are proportional to tangential and normal displacement components multiply by the frequency, respectively. In view of this, we combine the stresses and the grooved boundary conditions of the porous fibre-reinforced material with the tangential and normal displacement components in addition with the impedance term. The initial stress components are equally taken into account at the boundary and as part of application phenomena to this study Ailawalia et al [48], yielded (i) above when subjected

to mechanical force P_1. Z_1 and Z_2 are the impedance parameters. Hence, following the application of the boundary conditions (i-ii), we obtain the system of non-homogeneous algebraic equations below:

$$\{\{ibA_{16}-\nu_n H_{1n}A_{17}+H_{2n}\}+ab\sin bx_1\{(ibA_{13}H_{1n}-\nu_n A_{31})\} \\ +\{\omega H_{1n}Z_2+\mu_0 H_0^2(ib-\nu_n H_{1n})\}\}N_n e^{-\nu_n\eta(x_1)}=P_1/A_1, \tag{20}$$

$$\{\{ibH_{1n}-\nu_n\}A_{13}^*+ab\sin bx_1\{ib(1-(\mu_0 H_0^2/A_1))-\nu_n H_{1n}A_{16}+H_{2n}\} \\ +\{\omega Z_1\}\}N_n e^{-\nu_n\eta(x_1)+\omega t+ibx_1}=(abP/A_1)\sin bx_1, \tag{21}$$

$$\{(-\nu_n H_{2n})\}N_n e^{-\nu_n\eta(x_1)}=P_2/A_1. \tag{22}$$

$A_{13}^*=\mu_L/A_1,\ n=1,2,3.$

The above system of Equations (20-22); prescribes the solutions to the displacement components of the waves and stresses on the porous fibre-reinforced material with voids source and mechanical force when $N_n, n=1,2,3$ are found. If $P_1=P_2=P=0,$ the traction free grooved boundary conditions are achieved. When the Mechanical force and voids source are removed from the entire material, we observe that the introduction of the initially stressed parameter P has made the system of algebraic equations for the model to retain its non-homogeneous state as occasioned by the shear stress boundary conditions in (i) above i.e. the shear stress boundary condition which was in its free boundary state became non-homogeneous on introduction of the initial stress on the material.

5. Computational Results and Discussion

In this section we utilize the physical constants Othman et al [46], of fiber-reinforcements and other parameters as given below to study attributes of the material as it relates to its stresses and component of displacements occasioned by the effect of voids source, magnetic fields, mechanical force, grooved and impedance boundary parameters on the material. The analyses of the various behaviors of these field parameters are shown in Figures (1-9). This is sequel to the solutions of the equations of motion and dimensionless boundary conditions of the model given in this article at a constant time t.

Figure 1 depicts the effects on normal stress τ_{22}, shear stresses τ_{12}, τ_{21}, volume fraction field ϕ and the displacement components $u_i, i=1,2$ versus x_2 coordinate for varying wavenumber b associated with the grooved boundary. Also, this is when the magnetic fields H_0, mechanical force P_1, initial stress P, voids source P_2, impedance $Z_i, i=1,2$ and amplitude of the grooved boundary a parameters are constantly applied on the material. In view of this, it is obvious from Fig.1 that all the distribution functions attain their maximum in the range $0<x_2\le 0.75$. The displacement u_1, normal stress τ_{22} and the volume fraction fields ϕ tend to possess uniform behaviors in the range $6.5\le x_2\le 10$ along where their minimum amplitudes of distribution functions on the material tend to hold. u_2, and the shear stresses τ_{12} and τ_{21} have similar behaviors and the shear stresses would likely attain their minimum amplitude in the range $5.5\le x_2\le 10.$ However, an increase in the wavenumber $b,$ associated with the grooved boundary, decreases the amplitudes of the distribution functions on the material. These behaviors are uniformly decreasing in the range $6.5<x_2\le 10$ and $5.5\le x_2\le 10$ for u_1, normal stress τ_{22}, the volume fraction field ϕ and the shear stresses τ_{12} and τ_{21}, respectively. Also, mixed behaviors were observed for some of the distributions especially τ_{22} and ϕ in the range $0\le x_2<2.$ Owing from Fig 1, it physically entails that more wave numbers on the material boundary would reduce the displacements and modulations of surface waves on the material which in turn would reflect on the stresses applied to the considered structure.

Figure 2 entails the effects on normal stress τ_{22}, shear stresses τ_{12}, τ_{21}, volume fraction fields ϕ and the displacement components $u_i, i=1,2$ as against x_2 coordinate for distinct grooved boundary parameter a. This is such that the magnetic fields H_0, mechanical force P_1, initial stress P, voids source P_2, impedance $Z_i, i=1,2$ and wavenumber b, parameters are constant on the material. Hence, Fig. 2 demonstrates that all the distribution functions attain maximum amplitudes in the range $0 < x_2 \leq 1$. Almost all the given distributions tends to have uniform behaviors for $x_2 > 0$. The minimum amplitude of the distribution functions exists in the range $x_2 > 6$. In a different vein, an increase in the amplitude a of the grooved boundary increases the amplitudes of the distribution functions. This increase in behavior exists at certain points especially for $0 \leq x_2 \leq 6$. Physically, we could infer that the displacements or propagation of the waves happened along the grooved path at this instance.

Nevertheless, Fig. 3 depicts the effects on normal stress τ_{22}, shear stress τ_{12}, volume fraction fields ϕ and the displacement components $u_i, i=1,2$ versus x_2 coordinate for varying magnetic fields H_0, when the mechanical force P_1, initial stress P, voids source P_2, impedance $Z_i, i=1,2$ and grooved parameters are constant on the material. Thus, we observed that all the distribution functions attain their maximum amplitude of distribution in the range $0 \leq x_2 \leq 0.75$. They possess similar behaviors as in Fig.1. This is such that an increase in the magnetic fields H_0, completely decreases the amplitudes of the distribution functions as they ultimately attains uniform behavior between $6 \leq x_2 \leq 10$ where the minimum amplitudes for the respective distributions holds. This physically shows that the magnetic field is acting as a pull to the propagation of the waves, its displacements cum other distributions.

Furthermore, Fig 4 shows the behaviors of normal stress τ_{22}, shear stress τ_{12}, volume fraction field ϕ and the displacement components $u_i, i=1,2$ against x_2 coordinates for distinct initial stress P, when the mechanical force P_1, voids source P_2, impedance $Z_i, i=1,2$, magnetic fields H_0 and grooved parameters are constant on the material. Moreover, Fig. 4 stipulates that for $0 < x_2 \leq 0.5$, all the distribution functions attain their maximum amplitudes. They essentially demonstrate uniform behavior for $x_2 > 5.5$ where the minimum amplitude of the distribution functions exists except for u_2 whose minimum value of amplitude lies between $2 < x_2 \leq 10$. Be that as it may, an increase in the initial stress P on the material increases the amplitudes of the distribution functions. This increase in behavior exists at certain points especially for $0 \leq x_2 \leq 6$.

In addition, Fig 5 shows the behaviors of normal stress τ_{22}, shear stress τ_{12}, volume fraction fields ϕ and the displacement components $u_i, i=1,2$ versus x_2 coordinate for varying applied mechanical force P_1 when the initial stress P, voids source P_2, impedance $Z_i, i=1,2$, magnetic fields H_0 and grooved parameters are constant on the material. In addition, this is such that for $0 \leq x_2 < 0.8$, all the distribution functions attains their maximum amplitudes. They portray uniform behavior for $x_2 > 5.5$ where the minimum amplitude of the distribution functions occurs except for u_2 whose minimum value lies between $2 < x_2 \leq 10$. Also, an increase in the applied mechanical force P_1 on the plane surface of the fibre-reinforced material tends to increase the amplitudes of the distribution functions. This increase in behavior exists between $0 \leq x_2 \leq 6,$ and thus, this shows that the mechanical force is acting as a push on the material. Observe that Fig 4 and Fig 5 are similar but with striking difference in amplitude profiles for some of the field distributions.

Also, Fig 6 prescribes the effects of normal stress τ_{22}, shear stress τ_{12}, volume fraction fields ϕ and the displacement components $u_i, i = 1, 2$ versus x_2 for varying voids source P_2. Observe that this occurs when the initial stress $P,$ mechanical force P_1 , impedance $Z_i, i = 1, 2$, magnetic fields H_0 and grooved parameters are not varying on the material. Moreover, this is such that for $0 \leq x_2 < 8,$ all the distribution functions attains their maximum amplitudes of distributions. They present uniform behavior for $x_2 > 5.5$ where the minimum amplitude of the distribution functions occurs except for u_2 whose minimum value of amplitude lies between $2 < x_2 \leq 10$. Also, an increase in the voids source P_2 on the fibre-reinforced material increases the amplitudes of the distribution functions. This increase in behavior exists between $0 \leq x_2 \leq 6.$

In a similar manner, Fig 7 gives the variations of normal stress τ_{22}, shear stresses (τ_{12}, τ_{21}), volume fraction fields ϕ and the displacement components $u_i, i = 1, 2$ versus x_2 for varying impedance Z_1. In this instance, the initial stress $P,$ mechanical force P_1 , impedance Z_2, voids source P_2, magnetic fields H_0 and grooved parameters remains constant on the material. The distribution functions attain their maximum amplitudes in the range $0 \leq x_2 \leq 0.75.$ An increase in the impedance Z_1, shows no significant increase nor decrease in the amplitudes of the distribution functions of u_2, and shear stresses τ_{12} and τ_{21}; as they fast attains uniform behavior between $0 \leq x_2 \leq 10$. The minimum amplitudes for the respective distributions hold for $x_2 > 6$. Observe a very slight change in behaviors of u_1, τ_{22}, and voids ϕ between $0.25 \leq x_2 \leq 2.5.$ This shows that the impedance Z_1 is acting as a resistance to change for the given distribution functions on the material.

Consequently, Fig 8 stipulates the behaviors of normal stress τ_{22}, shear stresses τ_{12}, τ_{21}, volume fraction fields ϕ and the displacement components $u_i, i = 1, 2$ versus x_2 for varying impedance Z_2 when the mechanical force P_1, voids source P_2, impedance Z_1, magnetic fields H_0, initial stress $P,$ and grooved parameters are constant on the material. The distribution functions attain their maximum amplitudes in the range $0 \leq x_2 \leq 0.75.$ An increase in the impedance Z_2, essentially demonstrated neither increase nor decrease in the amplitudes of the distribution functions as they fast attained uniform behavior between $0 \leq x_2 \leq 10$. The minimum amplitudes for the respective distributions hold for $x_2 > 6$. This shows that the impedance Z_2 is acting as a mechanical resistance to change for the given distribution functions at every point on the material at this instance.

In a similar vein, Fig 9 demonstrates the variations of the normal stress τ_{22}, shear stresses (τ_{12}, τ_{21}), volume fraction fields ϕ and the displacement components $u_i, i = 1, 2$ against x_2 coordinate for varying fibre-reinforcement parameter α when the initial stress $P,$ mechanical force P_1 , impedances (Z_1, Z_2), voids source P_2, magnetic fields H_0 and grooved parameters are constant on the material. Fig 9 shows that for a decreasing reinforcement parameter α, all the distribution components of displacements, stresses and volume fraction fields on the material increases in modulation. The maximum distribution profiles of the displacement, stresses and voids, lies within the region of early impact of the waves on the material. However, the normal component of displacement has more impact of the reinforcement decrease. Physically, we can deduce that for a more reinforced structure, the modulation and impact of surface waves on the structure would be curtailed or decreased. This is owing to the decreasing effects of displacement and stresses on the structure for an increased reinforcement.

7. Conclusion

This study practically dealt on the analyses of surface waves in an initially stressed magneto-elastic material with voids source, corrugated and impedance boundary conditions influenced by an applied mechanical force on the surface of the material. In the light of this, we observe that these contributing physical parameters cum fields have remarkable degrees of influences on the propagation of the surface waves such that:

- An increase in the wavenumber b associated with the grooved boundary, decreases the distribution functions after attaining certain amplitudes. Uniform behaviors at certain points were equally recorded.
- An increase in the amplitude a of the grooved boundary increases the amplitudes of the distribution functions; displacements or propagation of the waves happened along the grooved path at this instance.
- The initial stress, voids source, and Mechanical force had an increased behavior to the distribution functions on the material when increased.
- An increase in the magnetic influences decreases the distribution profiles on the material.
- An increase in the impedance Z_2 gave neither increase nor decrease in the amplitudes of the distribution functions as they fast attained uniform behavior. This shows that the impedance Z_2 is acting as a mechanical resistance to change for the given distribution functions at every point on the material at this instance.
- A decrease in one of the reinforced parameter α, increases the distribution profiles of modulation of waves on the structure.

Physically, we can deduce that for a more reinforced structure, the modulation and impact of surface waves on the structure would be curtailed or decreased. Subsequently, this study also stipulates some considerable assertions such that more wave numbers associated with the grooved material boundary would reduce the modulations of surface waves on the considered medium. This in turn would reflect on the stresses applied to the considered structure whilst having high displacement around short distances across the material as vanishing and uniform effects are observed across further lengths on the material. In line with the combined effects of the physical parameters on the material, the magnetic fields acted as a pull affecting modulation of the surface waves on the structure. Also, the symmetric nature of the shear stresses on the material is evident and is depicted from this study especially from the given graphs. Thus, this research should be of great value to new researchers in the field and experimental based study involving wave propagations in a fibre-reinforced medium especially in computations likened to the dispersions and attenuations of surface waves.

References

[1] Spencer, A.J.M. "Deformations of fibre-reinforced materials", Oxford Uni. Pres. Lond. (1972). https://doi.org/10.1016/0010-4361(73)90757-X.
[2] Alam, P., Kundu, S., Badruddin, I. A., et al. "Dispersion and Attenuation

Characteristics of Love-Type Waves in a Fiber-Reinforced Composite over a Viscoelastic Substrate”, *Phys. Wave Phen.* **27**, 281–289 (2019). https://doi.org/10.3103/S1541308X19040083.

[3] Alam, P., Singh, K. S., Ali, R., et al. “Dispersion and attenuation of SH-waves in a temperature-dependent Voigt-type viscoelastic strip over an inhomogeneous half-space”, *ZAMM- J. Appl. Math. Mech*., **101**(12), (2021), https://doi.org/10.1002/zamm.202000223.

[4] Bounouara, F., Sadoun, M., Saleh, M. M. S., et al. “Effect of visco-Pasternak foundation on thermo-mechanical bending response of anisotropic thick laminated composite plates”, *Steel Compos. Struct.*, **47**(6), 693-707, (2023). DOI: 10.12989/scs.2023.47.6.693.

[5] Mario, J. S., and Alam, P. “A multi-layered model of Newtonian viscous liquid, fiber-reinforced and poro-elastic media over a self-weighted half-space to investigate the SH-wave interactions”, *Mech. Adv. Mater. Struc*., 1–13, (2023). https://doi.org/10.1080/15376494.2023.2256537

[6] M.A., Biot, “Mechanics of Incremental Deformations”, John Wiley and Sons, Inc.: New York, (1965).

[7] Abd-Alla, A.M., Abo-Dahab S.M. and khan, A. “Rotational Effects on Magneto-Thermoelastic Stoneley, Love and Rayleigh Waves in Fibre-Reinforced Anisotropic General Viscoelastic Media of Higher Order”, *CMC*., **53,** pp. 49–72 (2017). https://doi.org/10.3970/cmc.2017.053.052.

[8] Alam, P., Nahid, T., Al Alwan, B., et al. “Rotating radial vibrations in human bones (femoral, mandibular and tibia) and crystals (Mg, Co, Cd, Zn and beryl) made cylindrical shell under magnetic field and hydrostatic stress”, *Mech. Adv. Mater. Struc*., **30**(13), 2684–2700, (2023). https://doi.org/10.1080/15376494.2022.2062499

[9] Alam, P., Jena, S., Badruddin, I. A., et al. "Attenuation and dispersion phenomena of shear waves in anelastic and elastic porous strips", Eng. Comput., **38**(7), pp. 3132-3149, (2021). https://doi.org/10.1108/EC-07-2020-0381

[10] Cowin, S.C. and Nunziato, J.W. “Linear elastic materials with voids”, *J. Elast.*, **13**(2), 25-147 (1983). https://doi.org/10.1007/BF00041230.

[11] Venkatesan, P., Alam, P. A. “Multi-layered model of poroelastic, HSTI, and inhomogeneous media to study the Love-type wave propagation due to an impulsive point source a Green’s function approach”, *Acta Mech*., **235**, 409–428 (2024). https://doi.org/10.1007/s00707-023-03760-7

[12] Tahir, S. I., Chikh, A., Tounsi, A., et al. "Wave propagation analysis of a ceramic-metal functionally graded sandwich plate with different porosity distributions in a hygro-thermal environment", *Compos. Struct.*, **269**, 114030, (2021). https://doi.org/10.1016/j.compstruct.2021.114030

[13] Tahir, S. I., Chikh, A., Tounsi, A., et al. “The effect of three-variable viscoelastic foundation on the wave propagation in functionally graded sandwich plates via a simple quasi-3D HSDT”, *Steel Compos. Struct.*, **42**(4), 501, (2022). (DOI: 10.12989/scs.2022.42.4.501.

[14] Alsubaie, A. M., Alfaqih, I., Al-Osta, M. A., et al. I. “Porosity-dependent vibration investigation of functionally graded carbon nanotube-reinforced composite beam”, *Comput. Concr*, 32(1), 75-85. (2023). DOI:10.12989/cac.2023.32.1.075

[15] Asano, S. “Reflection and refraction of elastic waves at a corrugated interface”, *Bull. Seism. Soc. Am.*, **56**(1), pp. 201-221(1966). https://doi.org/10.1785/BSSA0560010201.

[16] Chowdhury, S., Kundu, S., Alam, P., et al. “Dispersion of Stoneley waves through the irregular common interface of two hydrostatic stressed MTI media”, *Scientia Iranica*, **28**(2), pp. 837-846 (2021). doi:10.24200/SCI.2020.52653.2820.

[17] Sadab, M., Kundu, S. “SH-wave propagation in a piezoelectric layer over a heterogeneous dry sandy half-space”, *Acta Mech.*, **234**(11), 5841–5854 (2023). https://doi.org/10.1007/s00707-023-03708-x

[18] Sadab, M. and Kundu, S. “SH-wave propagation in double layers imperfectly bonded over a dry sandy half-space”, *Int. J. Geomech.*, **23** (12), (2023). https://doi.org/10.1061/IJGNAI.GMENG-8698

[19] Singh, B. “Reflection of elastic waves from plane surface of a half-space with impedance boundary conditions”, Geoscience Research, **2**(4), pp. 242-253 (2017). https://dx.doi.org/10.22606/gr.2017.24004

[20] Maleki, F. and Jafarzadeh, F. “Model tests on determining the effect of various geometrical aspects on horizontal impedance function of surface footings”, *Scientia Iranica*, (2023).

doi:10.24200/SCI.2023.59744.6403.
[21] Singh, S. S. and Tomar, S. K. "qP-wave at a corrugated interface between two dissimilar pre-stressed elastic half-spaces", *J. Sound Vib.*, **317**(3), pp. 687-708 (2008). https://doi.org/10.1016/j.jsv.2008.03.036.
[22] Singh, A. K., Das, A., Kumar, S., et al. "Influence of corrugated boundary surfaces, reinforcement, hydrostatic stress, heterogeneity and anisotropy on Love-type wave propagation", *Meccanica,* 50(12), pp. 2977-2994 (2015). https://doi.org/10.1007/s11012-015-0172-6.
[23] Singh, A. K., Mistri, K. C., and Mukesh, P. K. "Effect of loose bonding and corrugated boundary surface on propagation of rayleigh-type wave", *Lat. Am. J. Solids Struct.,* **15**(1), e01, (2018). http://dx.doi.org/10.1590/1679-78253577.
[24] Das, S. C., Acharya, D. P. and Sengupta, D. R. "Surface waves in an inhomogeneous elastic medium under the influence of gravity", Rev Roumaine Sci. Tech. Ser Mec Appl., 37 pp. 539-551(1992).
[25] Abd-Alla, A. M., Abo-Dahab, S. M. and Alotaibi, H. A. "Effect of the Rotation on a Non-Homogeneous Infinite Elastic Cylinder of Orthotropic Material with Magnetic Field". *J. Comput. Theor. Nanosci.,* **13**(7), pp. 4476-4492(17) (2016). https://doi.org/10.1166/jctn.2016.5308.
[26] Roy, I., Acharya, D.P. and Acharya, S. "Propagation and reflection of plane waves in a rotating magneto-elastic fibre-reinforced semi space with surface stress". *Mech. & Mech. Eng*., **22**(4), 939–957, (2018) . DOI:10.2478/mme-2018-0074.
[28] Singh, B. and Sindhu, R. "Propagation of waves at interface between a liquid half- space and an orthotropic micropolar solid half-space", *Adv. Acoust. & Vib*., **2011,** pp. 1–5 (2011). https://doi.org/10.1155/2011/159437.
[29] Gupta, R.R. "Surface wave characteristics in a micropolar transversely isotropic half-space underlying an inviscid liquid layer", *Int. J. of Appl. Mech. Eng.,* **19**, pp. 49–60 (2014). https://doi.org/10.2478/ijame-2014-0005.
[30] Gupta, R.R. "Surface wave characteristics in a micropolar transversely isotropic half-space underlying an inviscid liquid layer", *Int. J. of Appl. Mech. Eng.,* 19, pp. 49–60 (2014). https://doi.org/10.2478/ijame-2014-0005.
[31] Anya, A.I., Akhtar, M.W., Abo-Dahab, M.S., et al. "Effects of magnetic field and initial stress on reflection of SV-waves at a free surface with voids under a gravity", *J. Mech. Behav. Mater.,* **27**, 5–6 (2018). https://doi.org/10.1515/jmbm-2018-0002.
[32] Anya, A.I., and Khan, A., "Reflection and propagation of plane waves at free surfaces of a rotating micropolar fibre-reinforced medium with voids", *Geomech. & Eng*., **18**(6), pp. 605–614 (2019). https://doi.org/10.12989/gae.2019.18.6.605.
[33] Anya, A.I., and Khan, A. "Reflection and propagation of magneto-thermoelastic plane waves at free surfaces of a rotating micropolar fibre-reinforced medium under G-L theory", *Int. J. of Acoust. & Vib.,* **25**(2), 190-199 (2020). https://doi.org/10.20855/ijav.2020.25.21575.
[34] Anya, A.I., and Khan, A. "Plane waves in a micropolar fibre-reinforced solid and liquid interface for non-insulated boundary under magneto-thermo-elasticity", *J. Comput. Appl. Mech.,* 53(2), pp. 204-218 (2022). DOI: 10.22059/JCAMECH.2022.341656.712.
[35] Sunita, D., Suresh, K.S. and Kapil, K.K. "Reflection at the free surface of fibre-reinforced thermoelastic rotating medium with two temperature and phase- lag", *Appl. Math. Model*., **65**, pp.106-19 (2019). https://doi.org/10.1016/j.apm.2018.08.004.
[36] Dey, S. and Addy, S.K. "Reflection of plane waves under initil stress at a free surface", *Int. J. Non-Linear Mech. Pergamon Press.*, **12**(6), pp. 371–381 (1977). https://doi.org/10.1016/0020-7462(77)90038-5.
[37] Nunziato, J.W. and Cowin, S.C. "A nonlinear theory of elastic materials with voids, *Arch. Rat. Mech. Anal.,* **72**(2), pp. 175-201(1979). https://doi.org/10.1007/BF00249363.
[38] Puri, P., and Cowin, S.C. "Plane waves in linear elastic materials with voids", *J. Elast*., **15**(2), pp. 167-183 (1985). https://doi.org/10.1007/BF00041991.
[39] Singh, B. and Kaur, B. "Rayleigh surface wave at an impedance boundary of an incompressible micropolar solig half-space", *Mech. Adv. Mater. Struct.,* **29**(25), pp. 3942-3949 (2022).

https://doi.org/10.1080/15376494.2021.1914795.
[40] Singh, B. and Kaur, B. “Rayleigh-type surface wave on a rotating orthotropic elastic half-space with impedance boundary conditions”, *J. Vib. Control.*, **26**(21-22), pp. 1980- 1987, (2020).
[41] Sahu, S.A., Mondal, S. and Nirwal, S. “Mathematical analysis of Rayleigh waves at the nonplanner boundary between orthotropic and micropolar media”, *Int. J. Geomech.*, **23**(3), (2022). doi.org/10.1061/IJGNAI.GMENG-7246.
[42] Giovannini, L. “Theory of dipole-exchange spin-wave propagation in periodically corrugated films”, *Phys. Rev. B,* 105(21), (2022). doi.org/10.1103/PhysRevB.105.214426.
[43] Rakshit, S., Mistri, K.C., Das, A., et al. “Effect of interfacial imperfections on SH-wave propagation in a porous piezoelectric composite”, *Mech. Adv. Mater. Struct.*, **29**(25), pp. 4008-4018 (2022). doi.org/10.1080/15376494.2021.1916138.
[44] Rakshit, S., Mistri, K.C., Das, A., et al. “Stress analysis on the irregular surface of visco-porous piezoelectric half-space subjected to a moving load”, *J. Intell. Mater. Syst. Struct*., **33**(10), (2021). https://doi.org/10.1177/1045389X211048226.
[45] Singh, S. S. and Tomar, S. K. “qP-wave at a corrugated interface between two dissimilar pre-stressed elastic half-spaces”, *J. Sound Vib.*, **317**(3), pp. 687-708 (2008). https://doi.org/10.1016/j.jsv.2008.03.036.
[46] Othman, M. I. A., Lotfy, K., Said, S. M., et al. “Wave propagation in a fiber-reinforced micropolar thermoelastic medium with voids using three models”, *Int. J. of Appl. Math. Mech.*, **8** (12), pp. 52-69 (2012).
[47] Azhar, E., Ali, H., Jahangir, A., et al. “Effect of Hall current on reflection phenomenon of magneto-thermoelastic waves in a non-local semiconducting solid”, *Waves in Random and Complex Media*. 1–18, (2023). https://doi.org/10.1080/17455030.2023.2182146.
[48] Ailawlia, P., Sachdeva, S. K. and Pathania, D. “A two dimensional fibre reinforced micropolar thermoelastic problem for a half-space subjected to mechanical force”, *Theor. Appl. Mech.*, **42** (1), pp. 11-25 (2015). DOI: 10.2298/TAM1501011A

Appendix

$$\mathrm{C1} = A_6 A_{13} A_{15};$$

$$\{(\rho A_{13}\left(F6A_9 - \left(A_7 + \omega\left(A_8 - \omega A_{10}\right)\right)A_{15}\right) - A_6(b^2 i^2 \rho A_{12}^2 + A_{15}(\rho\left(b^2+\omega^2\right)$$
$$+\omega^2 H_0^2 \varepsilon_0 \mu_0^2) + A_{13}\left(b^2\rho A_{14} + b^2\rho A_{15} + \omega^2\left(\rho + H_0^2\mu_0^2\right)\right)))\}/\rho;$$

$$C3 = \frac{1}{\rho^2}(A_6(b^4 i^2 \rho^2 A_{12}^2 + b^2\rho A_{13}(b^2\rho A_{14} + \omega^2\left(\rho + H_0^2\mu_0^2\right)) + \left(\rho\left(b^2+\omega^2\right) + \omega^2 H_0^2\varepsilon_0\mu_0^2\right)$$
$$\left(b^2\rho A_{14} + b^2\rho A_{15} + \omega^2\left(\rho + H_0^2\mu_0^2\right)\right)) + \rho(-F6A_9(b^2\rho + \rho\omega^2 + 2b^2 i^2\rho A_{12}$$
$$-b^2 i^2 \rho A_{15} + \omega^2 H_0^2\varepsilon_0\mu_0^2) + \left(A_7 + \omega\left(A_8 - \omega A_{10}\right)\right)(b^2 i^2 \rho A_{12}^2 +$$
$$A_{15}\left(\rho\left(b^2+\omega^2\right) + \omega^2 H_0^2\varepsilon_0\mu_0^2\right) + A_{13}\left(b^2\rho A_{14} + \omega^2\left(\rho + H_0^2\mu_0^2\right)\right))));$$

$$C4 = -\{\left(b^2\rho A_{14} + \omega^2\left(\rho + H_0^2\mu_0^2\right)\right)(b^2\rho\omega A_8 + \rho\omega^3 A_8 + b^2 F6 i^2 \rho A_9 - b^2\rho\omega^2 A_{10} - \rho\omega^4 A_{10}$$
$$+\omega^3 A_8 H_0^2\varepsilon_0\mu_0^2 - \omega^4 A_{10} H_0^2\varepsilon_0\mu_0^2 + b^2 A_6\left(\rho\left(b^2+\omega^2\right) + \omega^2 H_0^2\varepsilon_0\mu_0^2\right) +$$
$$A_7\left(\rho\left(b^2+\omega^2\right) + \omega^2 H_0^2\varepsilon_0\mu_0^2\right))\}/\rho^2$$

Biography

Dr. Augustine Igwebuike Anya holds a PhD in Mathematics with a research major in Solid Mechanics which involves Mathematical modeling of phenomena cum propagation in elastic materials/media with fluid interactions, from COMSATS University Islamabad, in 2021. He is also, 2016 The World Academy of Sciences and COMSATS University Islamabad (TWAS-CUI) PhD fellow in Mathematics. He won a merit based NMC-CIIT scholarship as one of the top 20 participants after a competition in National Graduate Training and Development Programme/Foundation Post-Graduate Courses (FPC) at National Mathematical Centre (NMC), Abuja, Nigeria in 2013, for a Post-Graduate study in MS Mathematics in 2014 at COMSATS Institute of Information Technology (CIIT), Islamabad, now COMSATS University Islamabad. He graduated with a Second Class (Hons.) Upper Division in BSc. Mathematics from the University of Abuja, Nigeria, and was the second best graduating student in the Department of Mathematics for the class of 2009/2010 session.
He is currently a Lecturer in Mathematics at the Veritas University Abuja, Nigeria.

Figure Captions

Figure 1**:** The distribution of displacement components $u_i, i = 1, 2$, normal stress τ_{22}, shear stresses τ_{12}, τ_{21}, and volume fraction field ϕ versus x_2 in meters for distinct values of wavenumber b.
Figure 2**:** The distribution of displacement components $u_i, i = 1, 2$, normal stress τ_{22} shear stresses τ_{12}, τ_{21} and volume fraction field ϕ versus x_2 in meters for distinct values of grooved parameter a.
Figure 3: The distribution of displacement components $u_i, i = 1, 2$, normal stress τ_{22} shear stresses τ_{12}, τ_{21}, and volume fraction field ϕ versus x_2 in meters for distinct values of magnetic field H_0.
Figure 4**:** The distribution of displacement components $u_i, i = 1, 2$, normal stress τ_{22} shear stresses τ_{12}, τ_{21}, and volume fraction field ϕ versus x_2 in meters for distinct values of initial stress P in N / m^2.
Figure 5: The distribution of displacement components $u_i, i = 1, 2$, normal stress τ_{22} shear stresses τ_{12}, τ_{21}, and volume fraction field ϕ versus x_2 in meters for distinct values of mechanical force P_1 in Newton.
Figure 6: The distribution of displacement components $u_i, i = 1, 2$, normal stress τ_{22} shear stresses τ_{12}, τ_{21}, and volume fraction field ϕ versus x_2 in meters for distinct values of voids source P_2.
Figure 7: The distribution of displacement components $u_i, i = 1, 2$, normal stress τ_{22} shear stresses τ_{12}, τ_{21}, and volume fraction field ϕ versus x_2 in meters for distinct values of impedance parameter Z_1.
Figure 8: The distribution of displacement components $u_i, i = 1, 2$, normal stress τ_{22}, shear stresses τ_{12}, τ_{21}, and voids ϕ versus x_2 in meters for distinct values of impedance parameter Z_2.
Figure 9: The distribution of displacement components $u_i, i = 1, 2$, normal stress τ_{22}, shear stresses τ_{12}, τ_{21}, and voids ϕ versus x_2 in meters for distinct values of a fibre-reinforced parameter α.

Figures

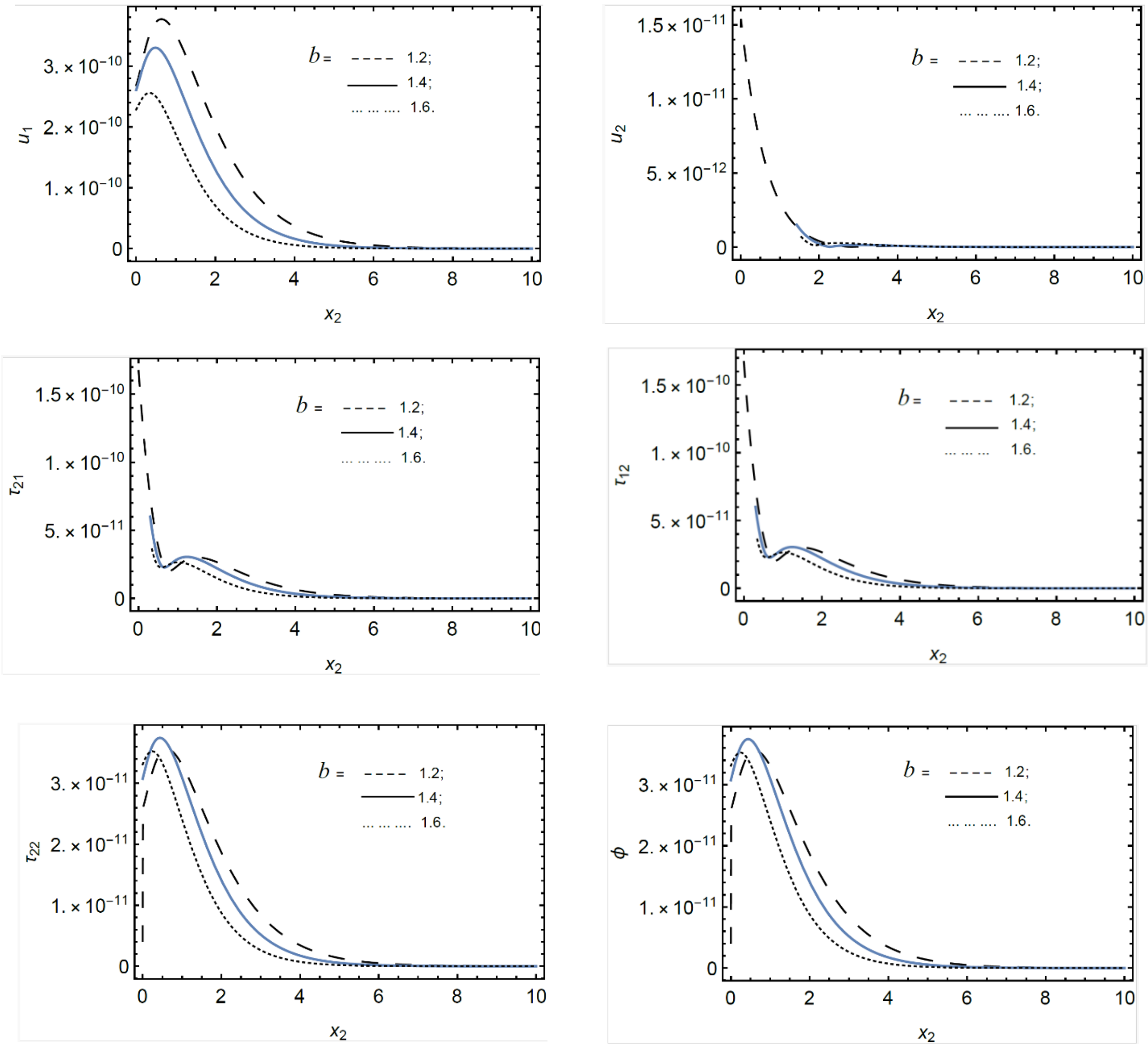

Figure 1

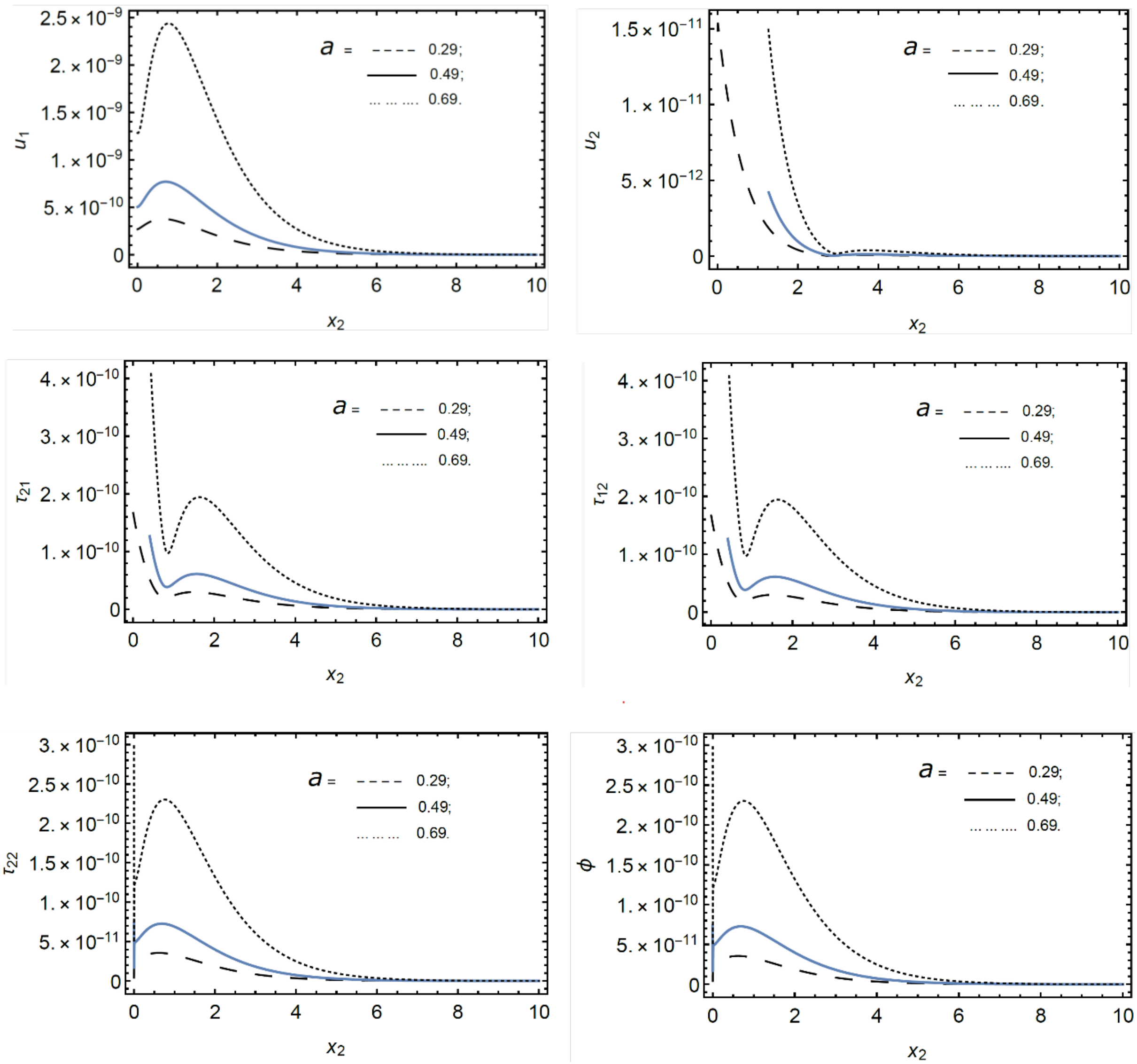

Figure 2

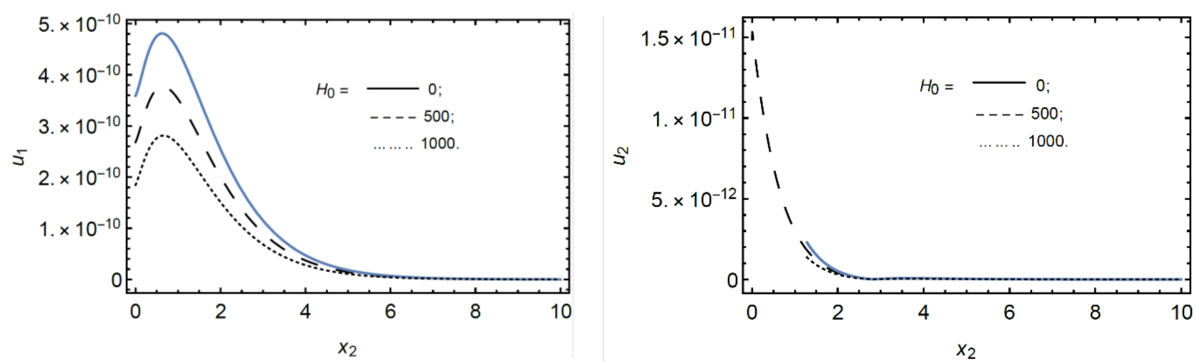

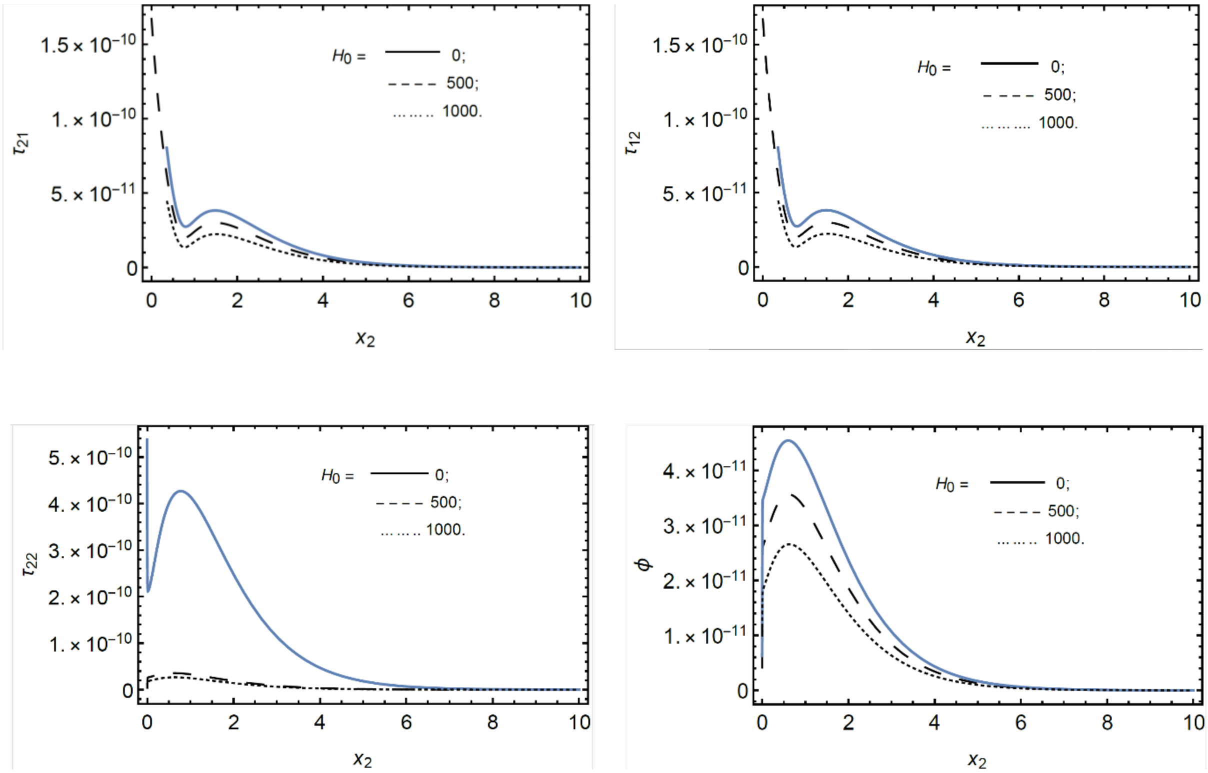
τ_{21}
H_0 = 0; 500; 1000.
x_2
τ_{12}
H_0 = 0; 500; 1000.
x_2
τ_{22}
H_0 = 0; 500; 1000.
x_2
ϕ
H_0 = 0; 500; 1000.
x_2

Figure 3

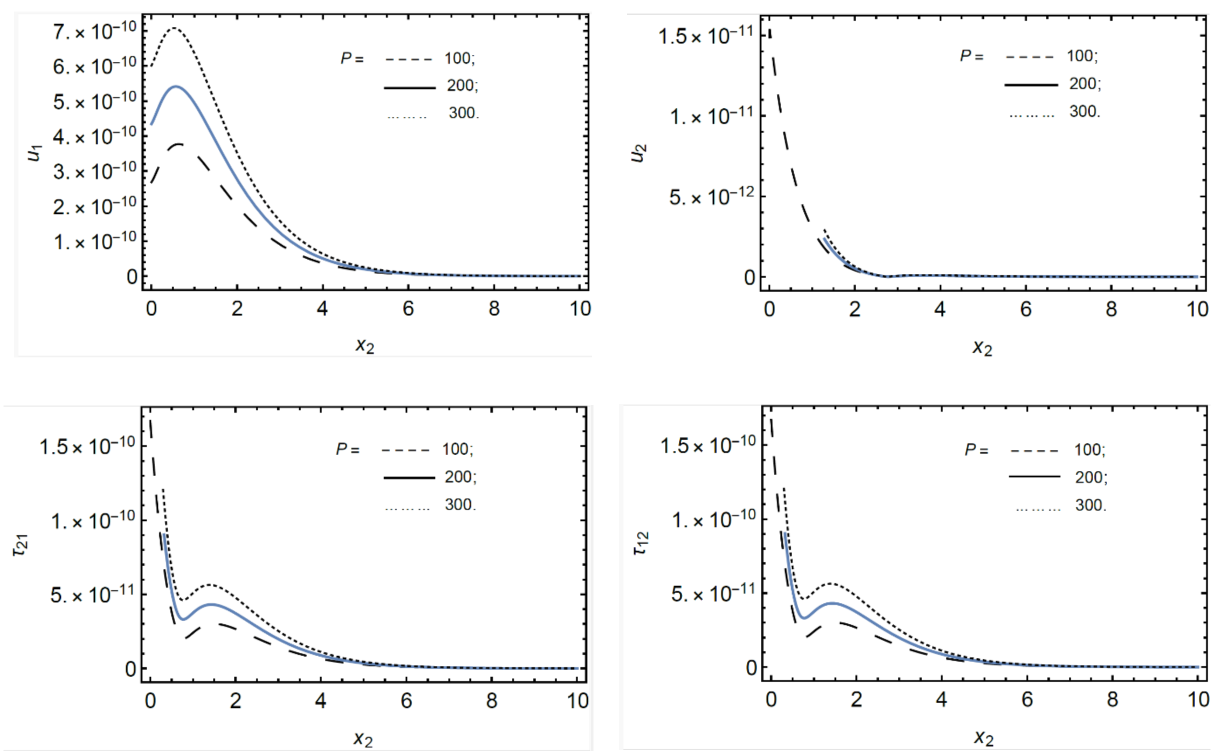
u_1
P = 100; 200; 300.
x_2
u_2
P = 100; 200; 300.
x_2
τ_{21}
P = 100; 200; 300.
x_2
τ_{12}
P = 100; 200; 300.
x_2

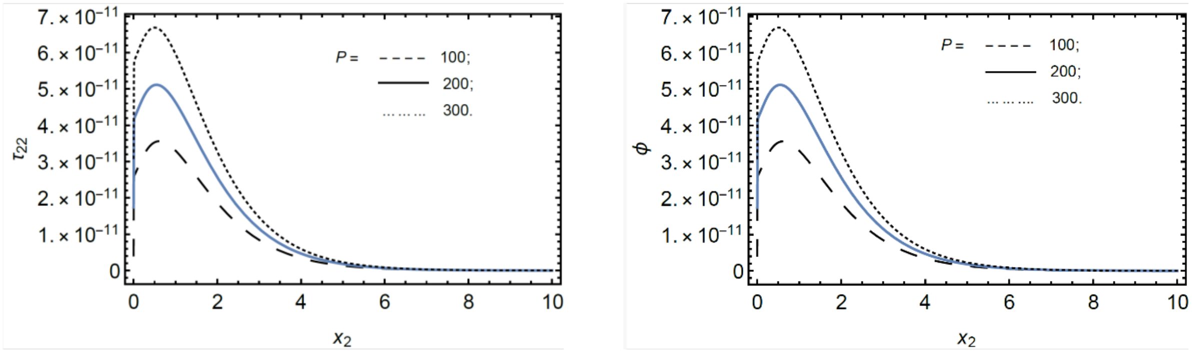

Figure 4

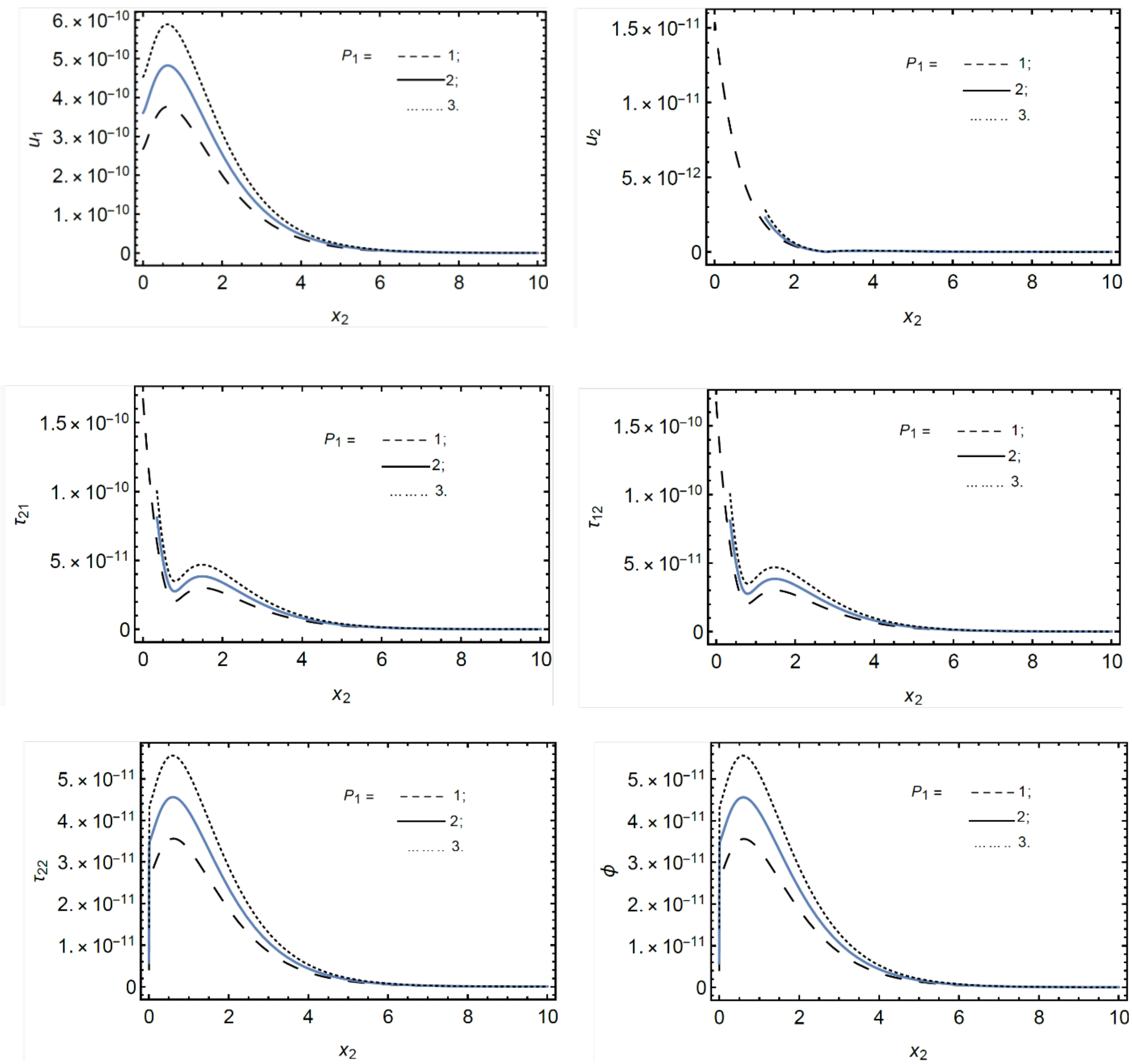

Figure 5

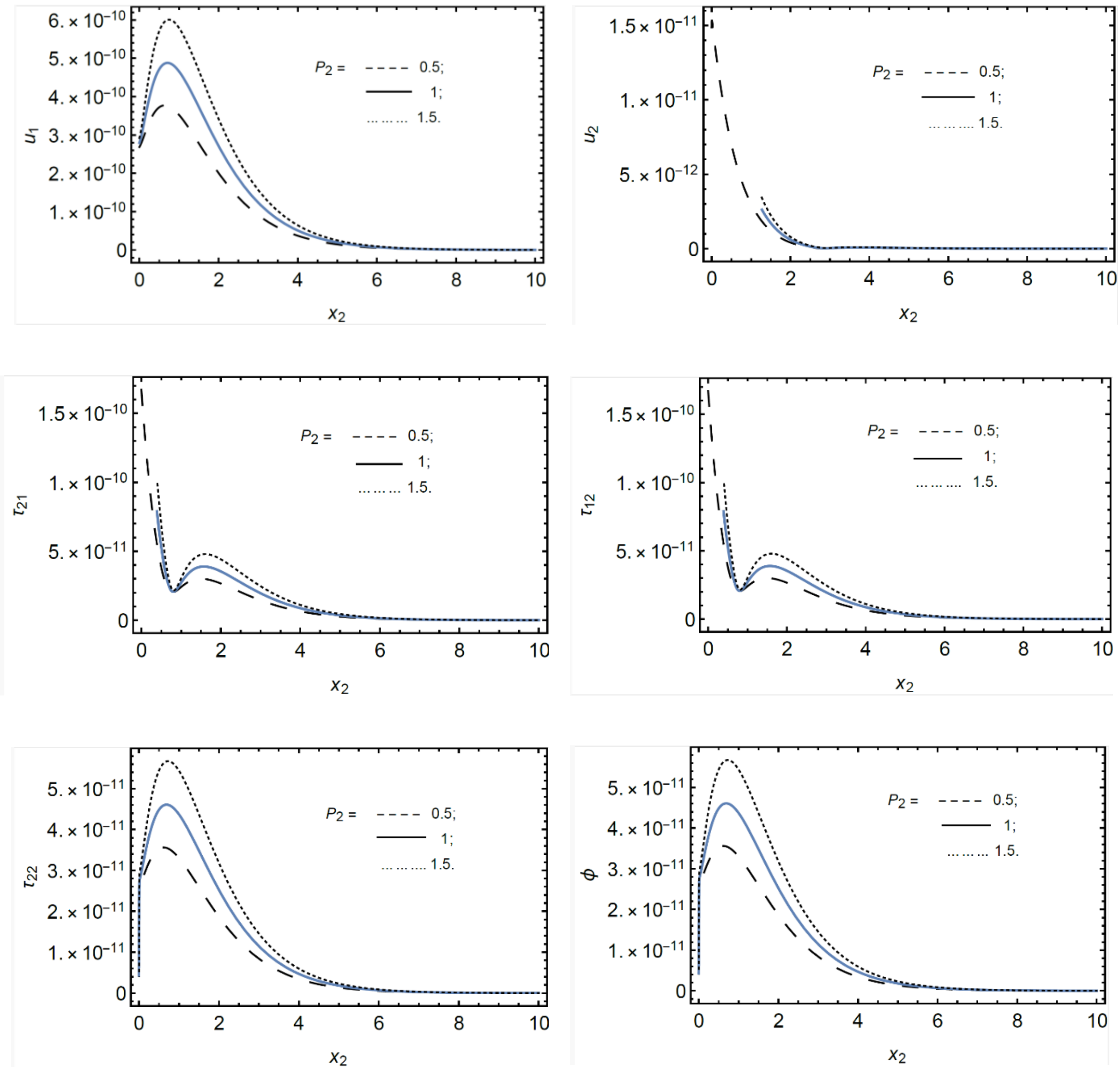

Figure 6

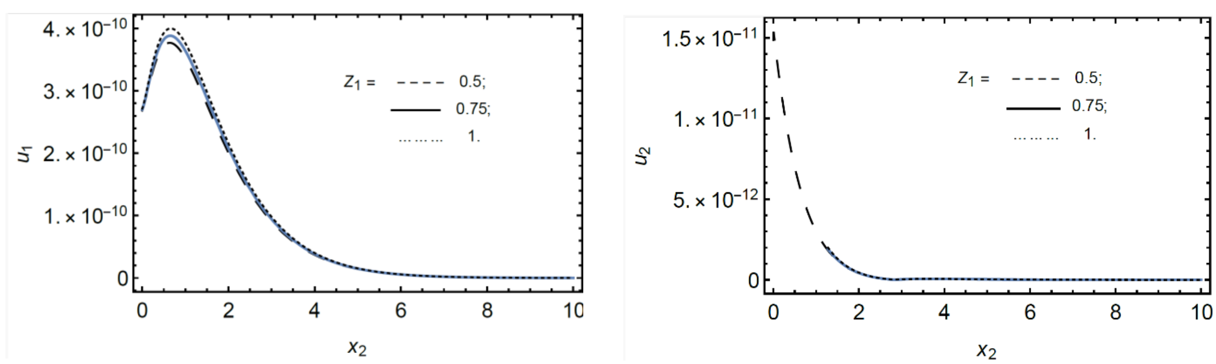

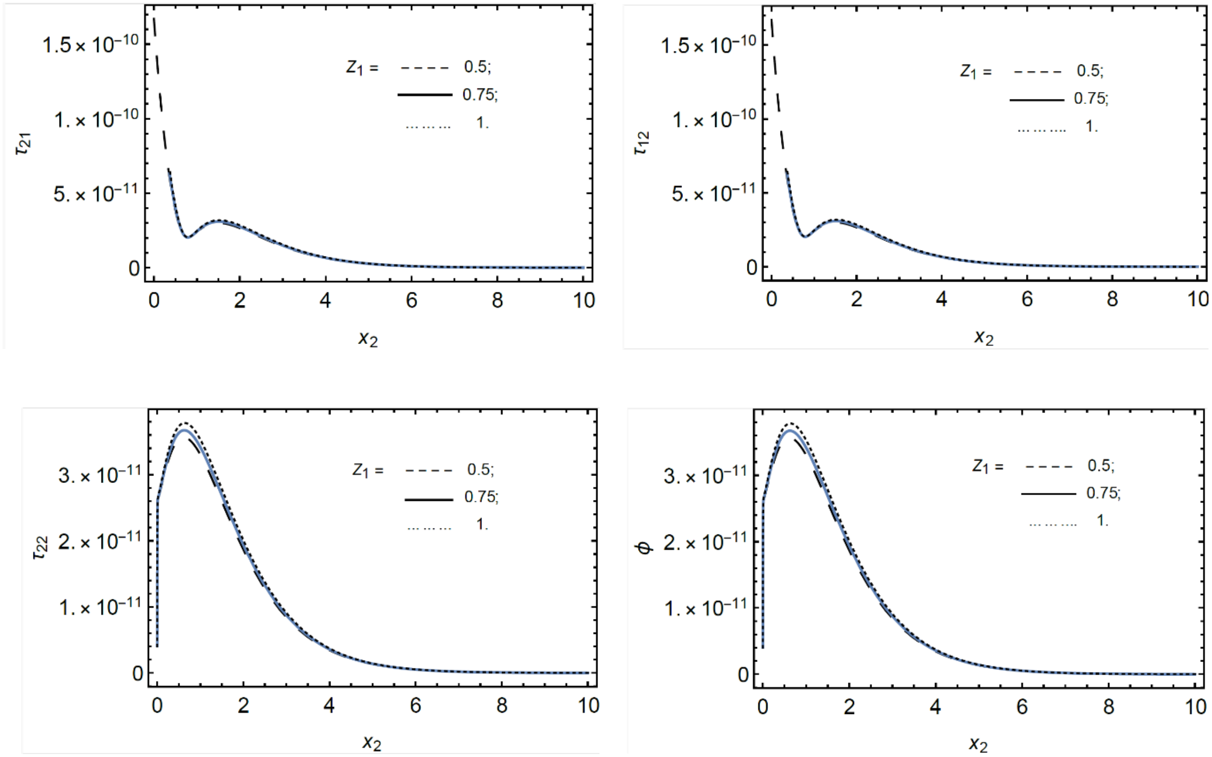
τ21
x2
Z1 = 0.5; 0.75; 1.
τ12
τ22
ϕ
1.5 × 10^-10
1. × 10^-10
5. × 10^-11
3. × 10^-11
2. × 10^-11
1. × 10^-11
0
2
4
6
8
10

Figure 7

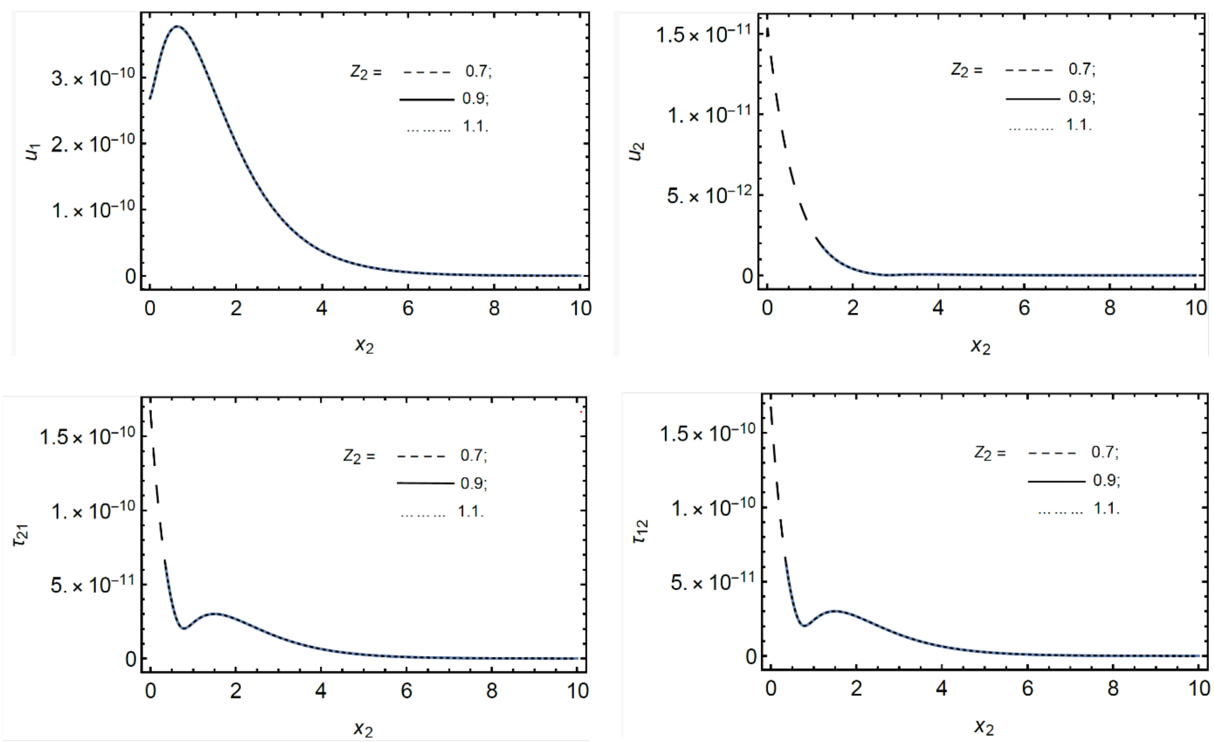
u1
u2
τ21
τ12
x2
Z2 = 0.7; 0.9; 1.1.
3. × 10^-10
2. × 10^-10
1. × 10^-10
1.5 × 10^-11
1. × 10^-11
5. × 10^-12
1.5 × 10^-10
5. × 10^-11
0
2
4
6
8
10

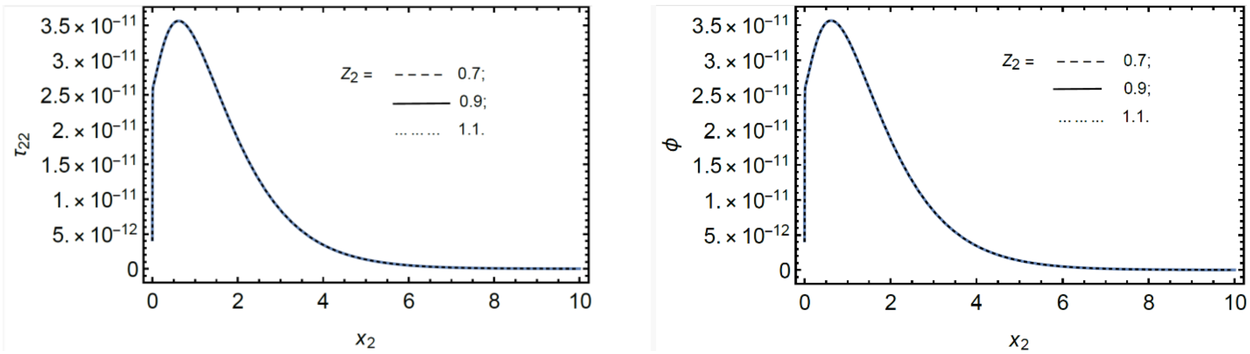

Figure 8

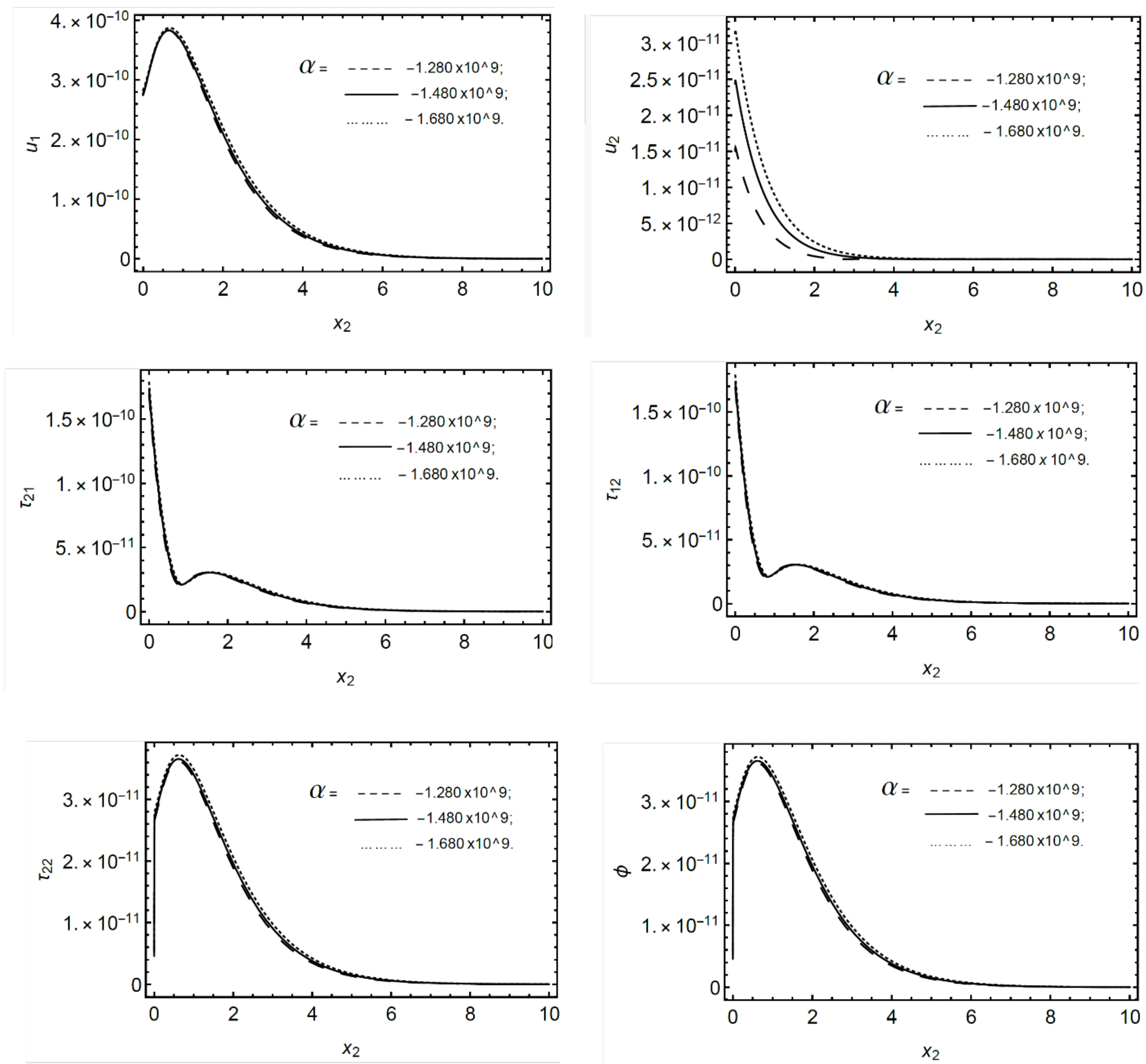

Figure 9